DOI: 10.13009/EUCASS2025-170
11TH EUROPEAN CONFERENCE FOR AERONAUTICS AND SPACE SCIENCES (EUCASS)

INSULATION OPTIMIZATION OF DUAL-FOAM INSULATED H2 CRYOGENIC TANK

Carles Oliet[⋆†], *Eugenio Schillaci*[⋆], *Marcial Mosqueda-Otero*[⋆], *Ahmad Amani*[⋆], *Joaquim Rigola*[⋆] *and Jesús Castro*[⋆]
[⋆] *Heat and Mass Transfer Technological Center (CTTC), Universitat Politècnica de Catalunya (UPC)*
08222 Terrassa, Spain, https://www.cttc.upc.edu
carles.oliet@upc.edu · eugenio.schillaci@upc.edu · ahmad.amani@upc.edu · joaquim.rigola@upc.edu · jesus.castro@upc.edu
[†]Corresponding author

Abstract

This paper presents a numerical study to identify the best insulation thicknesses for a dual-foam based aircraft LH_2 tank. The simulation combines a 0D non-equilibrium model for the fluid and a multilayered 1D model for the insulation. The results identify the insulation combinations which accomplish a particular dormancy time, while keeping temperature sensitive materials in safe operation for a wide range of ambient temperatures. Among the acceptable insulations, additional KPIs like gravimetric parameters are incorporated to find the optimal solutions. Scalability effects are finally shown by applying the same methodology to different tank sizes.

1. Introduction

Cryogenic tank insulation is critical in minimising heat transfer in such an extreme temperature application. Relevant technologies for their construction were already identified in the 2000s,[11] and no relevant recent updates have been identified.[14] Key technologies include vacuum insulation, multilayer insulation (MLI), powder insulation, and foam insulation, often combined to obtain complex insulation assemblies. The dominant current technology is based on high-vacuum insulation (Dewar tank design), which eliminates gas convection and conduction, and is often combined with Multilayer Insulation (MLI), consisting of several layers of low-emittance, metal-coated sheets and low-conductivity spacers (e.g., glass fibres) to minimise radiation gains. Powder insulation uses low-density powders (e.g., perlite) to disrupt solid and gas conduction, and requires also vacuum. Finally, foam insulation employs lightweight porous materials with moderate thermal conductivity but no need of vacuum. The Dewar vacuum-based cryogenic tank has two main weaknesses: i) it is relatively heavy due to the double-layer metallic wall and the pressure difference requirements; ii) any event which eliminates the vacuum level has a critical impact on the insulation gains.[13] For ground-stationary or even for road transport, an eventual emergency situation can be managed by boil-off or safety/emergency measures. However, for an aircraft, this could create a strong risk, as potentially losing all the fuel in zones far from any emergency landing option. Under this framework, and also looking for potential gains in gravimetric index and geometry flexibility, there is an increasing interest in the use of foams to substitute or complement the Dewar conventional design. Hastings et al.[8] added a closed cell insulation layer (referenced as SOFI) between the inner tank and the MLI, in order to increase the vacuum space surface temperatures, allowing purging with N_2 instead of He. Fesmire et al.,[5] highlighted the potential uses of aerogel open cell foams for cryogenic insulation, and analysed experimentally their behaviour at different pressures (from vacuum to atmospheric conditions) and interstitial presence of different gases, confirming a strong effect of both on the thermal conductivity. In this context, the project H2ELIOS is doing research to demonstrate the feasibility of a tank inspired on a dual-foam insulation concept (patented by Cimadevilla and Ortega[4]). Regarding the selection of materials and their temperature constraints, several limitations have already been identified. The concerns on the closed cell long-term damage at cycling LH_2 temperature levels (already reported by Anthony et al.[2]) and the lack of certification/information of the materials under those conditions are a first aspect to consider. Secondly, the behaviour of the open cell material in the presence of a gas filler, and its performance at different temperatures and pressures, is also a crucial aspect for the insulation layout. Finally, for the structural carbon fibre reinforced polymer (CFRP) layer between both insulations, some concerns have also been identified on its operation at LH_2 temperatures, due to micro-crackings derived from extreme temperature changes and CTE misalignment in different directions within the material,[6,10] creating potential leakage.

This paper is devoted to showing the suggested methodology for the selection of the two insulation layers, in terms of materials and thicknesses, addressing the dormancy and safe interface temperature requirements. After the identification of the feasible thickness combination perimeter, additional KPIs can be added to the analysis for the selection of

DOI: 10.13009/EUCASS2025-170

the best candidates. Most results are focused on a reference tank, but additional content is given to show the use of the methodology to assess the scalability behaviour of the dual-foam concept.

2. Numerical models

The applied numerical models for this particular study have been selected to be computationally efficient, in order to extend easily the scope of these preliminary tests (different thicknesses, ambient temperatures and tank sizes), while keeping the physical representativeness. A 0D non-equilibrium model for the fluid, already implemented in a Digital Twin[12] developed by the authors, and a 1D model for the insulation skin have been combined in this framework.

2.1 Fluid

The 0D non-equilibrium model, similar to the approach by Al Ghafri et al.,[1] independently models the vapor and liquid as two control volumes. These zones are coupled by interface conditions (depicted in Figure 1) and interact with mass flows from charging, discharging, or venting. Heat transfer is incorporated from insulation and thermal bridges (using a factor from 3D simulations), along with any electric heaters in the liquid. NIST-REFPROP[9] provides the temperature and pressure-dependent thermal properties for H_2; dedicated functions have also been implemented for solid materials.

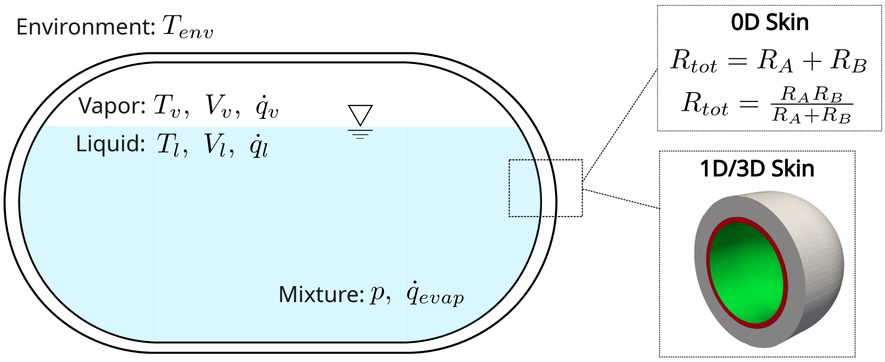

Figure 1: 0D non-equilibrium model scheme.

Convective heat transfer from the walls is modelled using empirical correlations for pool boiling and natural convection. At the liquid-vapour interface, heat transfer is determined by a specialised, physics-based buoyancy-corrected correlation. This correlation was calibrated against a broad range of dormancy cases from literature, including work by Aydellot[3] and Hasan et al.[7]

2.2 Insulation

The available Digital Twin[12] allows using different skin models, from 0D to 3D. Considering the focus of this study, the 3D model is not adding value, as the insulation thickness determination is not considering any multidimensional constructive details like supports, etc. On the other hand, the 0D model, which assumes a single thermal resistance per layer, loses the capability to integrate local changes in thermal conductivity due to temperature variation. Then, even though the results shown in this paper keep constant thermal conductivities under steady state conditions, the general methodology needs a 1D finite volume numerical integration (Figure 2) of the transient heat conduction equation (Equation 1) in the radial direction. The complete tool would allow, in future additional studies, to capture with moderate computational time transient effects and variable properties with temperature.

$$\rho c \frac{\partial T}{\partial t} = \nabla \cdot k \nabla T + \dot{q}_v \tag{1}$$

2.3 Combined approach towards optimization/design

The study described in the following sections investigates the trade-off to comply with the dormancy requirement with the lowest insulation thickness (and the best dual-foam thickness combination), while keeping the sensitive materials above their limit temperature. For this particular study, the calculation has been split into two parts, trying to set

DOI: 10.13009/EUCASS2025-170

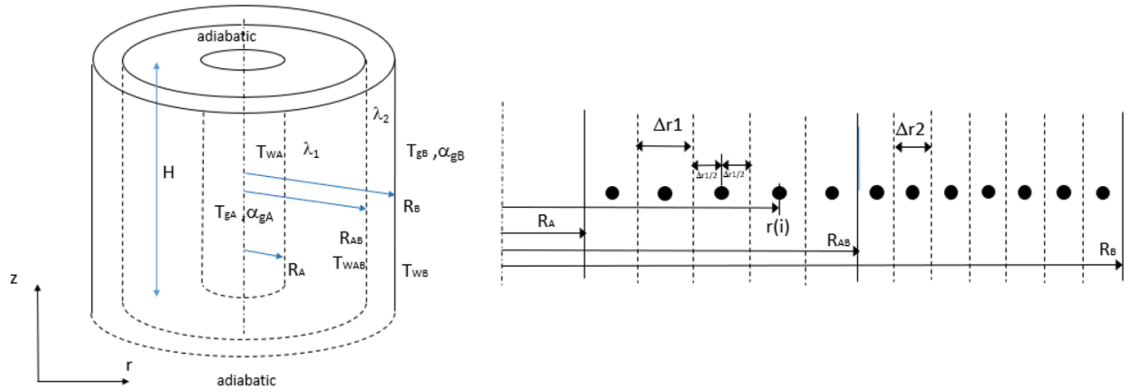

Figure 2: 1D skin model approach and corresponding discretisation.

up a computationally lighter methodology than applying routinely the coupled insulation-fluid approach available in the developed Digital Twin.[12] The first part would extract the tank dormancy behaviour when applying different heat flux levels, obtained by a much reduced number of cases with varying insulation level and adding thermal bridges from previous analysis. The second part is a systematic parametric study of dual-foam insulation thicknesses for each tank size, changing also the ambient temperature, which allows to identify the obtained heat flux and foams interface temperature for each case.

3. Results

3.1 Case description

The reference tank geometry under study is cylindrical with semi-spherical domes, and is placed horizontally. Starting conditions of 1 bar at saturation and a venting pressure of 6 bar have been considered for the dormancy studies. Regarding the application of such a concept to different commercial aircraft ranges, tentative sizes have been defined (Table 1), while taking the smallest one (S1) as the reference.

Table 1: Tank sizes considered to analyse scalability.

Tank	S1	S2	S3	S4	S5	S6
Volume (m^3)	3.0	5.5	7.3	9.1	20.1	40.2

The tanks envelope is composed of different layers, covering insulation, mechanical, protection and vapour barrier purposes. Regarding this study, the two most important layers that are intended to be analysed to obtain design conclusions are the insulations outside (ext) and inside (int) the CFRP tank.

The ambient temperature obviously takes a prominent role in an insulation study. The higher the worse in general, as it increases the gains and reduces the dormancy. However, in this study, attention must also be paid to the lowest temperature range, as it is the one potentially limiting by the minimum operating temperatures of the insulations and the outer tank. Taking into account the overall operation of the tank and possible accidental events, the range is taken between $-55°C$ up to $80°C$.

Due to confidentiality issues, in the current paper the properties of the two foams cannot be shared, and are described by a fixed ratio of thermal conductivities ($k_{int}/k_{ext} = 2$) and densities ($\rho_{int}/\rho_{ext} = 2$), without a direct link with actual/definitive material properties. The focus of the paper is to show the developed methodology and the design conclusions that can be extracted.

3.2 Dormancy vs heat flux

As commented above, the first step of the proposed methodology is to characterise the response of the different tanks under analysis under varying heat ingresses. This is done using the 0D non-equilibrium model for a pressurisation case from 1 to 6 bar, the pressure level when the tank starts venting. The representative result of each case would be

DOI: 10.13009/EUCASS2025-170

the dormancy time vs. the applied heat. In order to progress with the second part of the simulation, it is of particular interest to consider the heat flux in the cylindrical liquid zone of the tank. Figure 3 shows the obtained results for the six different tank sizes under analysis, highlighting the scale effect in the extension of dormancy times for the same insulation heat fluxes (volume vs surface ratio), or the extended heat allowable for fixed dormancy.

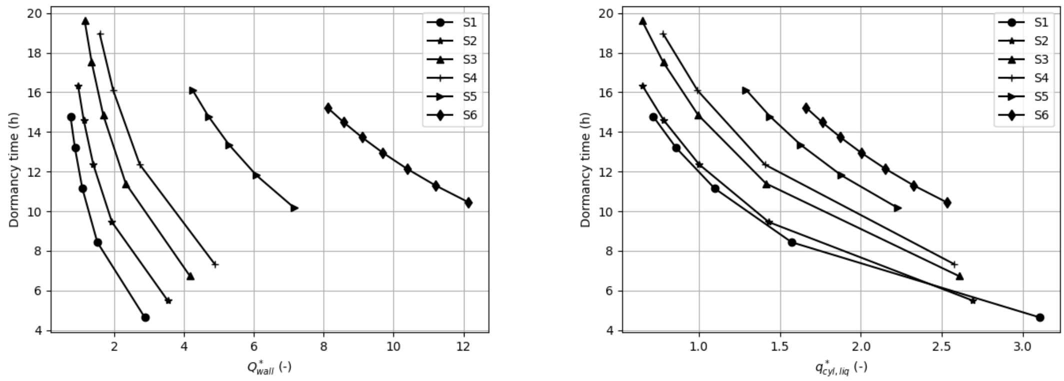

Figure 3: Dormancy vs heat ingress analysis for different tank sizes.

At this point, the dormancy objective is established as 12 hours, aligned with a conservative overnight period of inactivity of the aircraft at the airport facilities. From the available results, the corresponding limiting heat flux at the cylindrical area in contact with the liquid has been determined to progress with the insulation study in the following section. For the confidentiality mentioned above, the results are non-dimensionalised, taking the S1 tank at 12h dormancy as the reference.

3.3 Insulation thicknesses

The simultaneous change in the thicknesses of both insulations has been carried out by using the 1D multilayer simulation tool in cylindrical geometry, fixing the corresponding external ambient temperature and the LH_2 temperature.

The obtained heat flux and the outer tank temperature have been extracted and are reported in a matrix-like way depending on the two insulator thicknesses, for the two limiting ambient temperatures (Figure 4). The values are non-dimensionalised by the dormancy limiting heat flux and by the interface admissible temperature level. The heat flux patterns show the expected reduction with the increase of both thicknesses, with a bias to the internal foam as having the highest thermal conductivity. The impact of the ambient temperature is identified by an overall increase in the heat flux values for the highest outdoor condition, while keeping the same trends. Regarding the interface outer tank temperature, the pattern is dependent on the relative share of both foams in the overall insulation thermal resistance. In this case, the lowest ambient temperature is the one creating lower interface temperature values, thus becoming the limiting case for this constraint. In order to better observe the limits where the two opposite objectives are fulfilled, Figure 5 recolours the results as positive (green) or negative (red) cases for the heat flux limit and for the outer tank temperature threshold. The maximum ambient temperature, as expected, is the one producing higher heat transfer rates, thus moving the heat flux limiting operational frontier upwards. Conversely, it can be observed how the minimum ambient temperature is the most restrictive for the interface temperature, moving the corresponding limiting green/red operational frontier to the right.

For each ambient temperature, the combination of the green area on heat flux and outer tank temperature generates the feasible insulation combination perimeter. Figure 6 shows simultaneously the perimeters for the minimum and maximum ambient temperatures. The top-right zone with overlapping symbols and green colour fulfils at the same time the two design constraints for the two limiting ambient conditions, thus becoming the acceptable design envelope.

From this analysis, one could easily understand that the most convenient design points would be placed in the areas with the lowest internal and external insulation thicknesses, which saves weight and cost. However, this general observation is not enough to decide which particular thickness combination is the best. Therefore, an additional assessment should be done in terms of installation constraints, cost and/or gravimetric index to finally select the best int+ext thicknesses for a particular tank size. A complete design selection process is being done at the project level, considering several constraints. In this paper, and as an illustrative exercise, a gravimetric parameter (GP) has been defined (Equation 2) in

DOI: 10.13009/EUCASS2025-170

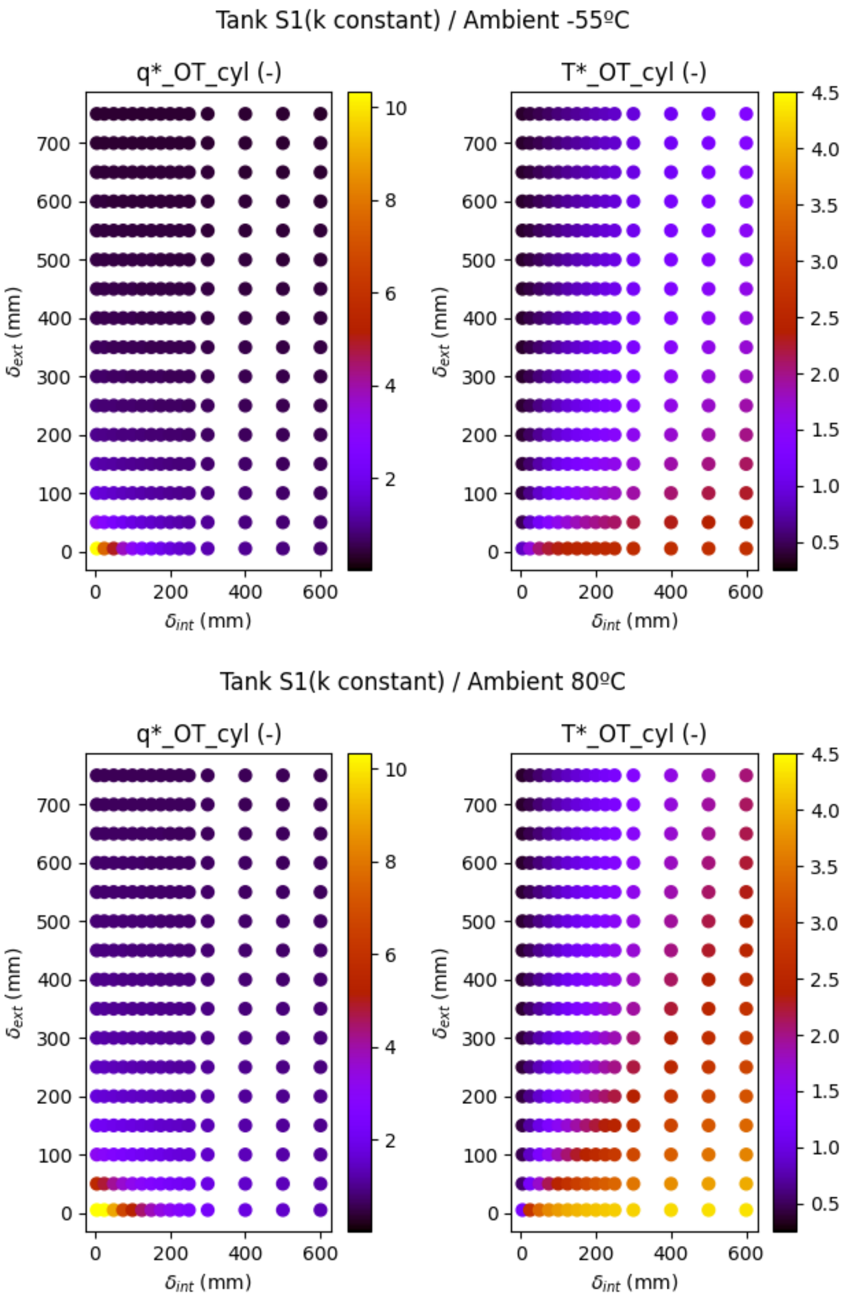

Figure 4: Insulation thickness impact on non-dimensional heat flux and outer tank temperature, for minimum (top) and maximum (bottom) ambient temperatures.

order to show, on the selected insulation envelope, an additional assessment in terms of weight.

$$GP = \frac{\rho_{int}\delta_{int} + \rho_{ext}\delta_{ext}}{m_{H2}} \tag{2}$$

Figure 7 shows how the S1 tank gravimetric parameter evolves in the identified insulation feasible zone. As observed in the left-hand graph, the obvious trend of decreasing GP with thickness is observed. The right-hand graph shows a zoom of the best area, in this particular case showing the best candidate (δ_{int}=200 mm and δ_{ext}=350 mm) under this criterion.

The observed large thicknesses for this best S1 design suggest that for such a scale, the solution is probably of difficult implementation due to weight and cost penalties. This conclusion is obviously related to the considered insulation properties, and particularly to the limits fixed on the dormancy time and the extreme ambient temperatures. Thus, first,

DOI: 10.13009/EUCASS2025-170

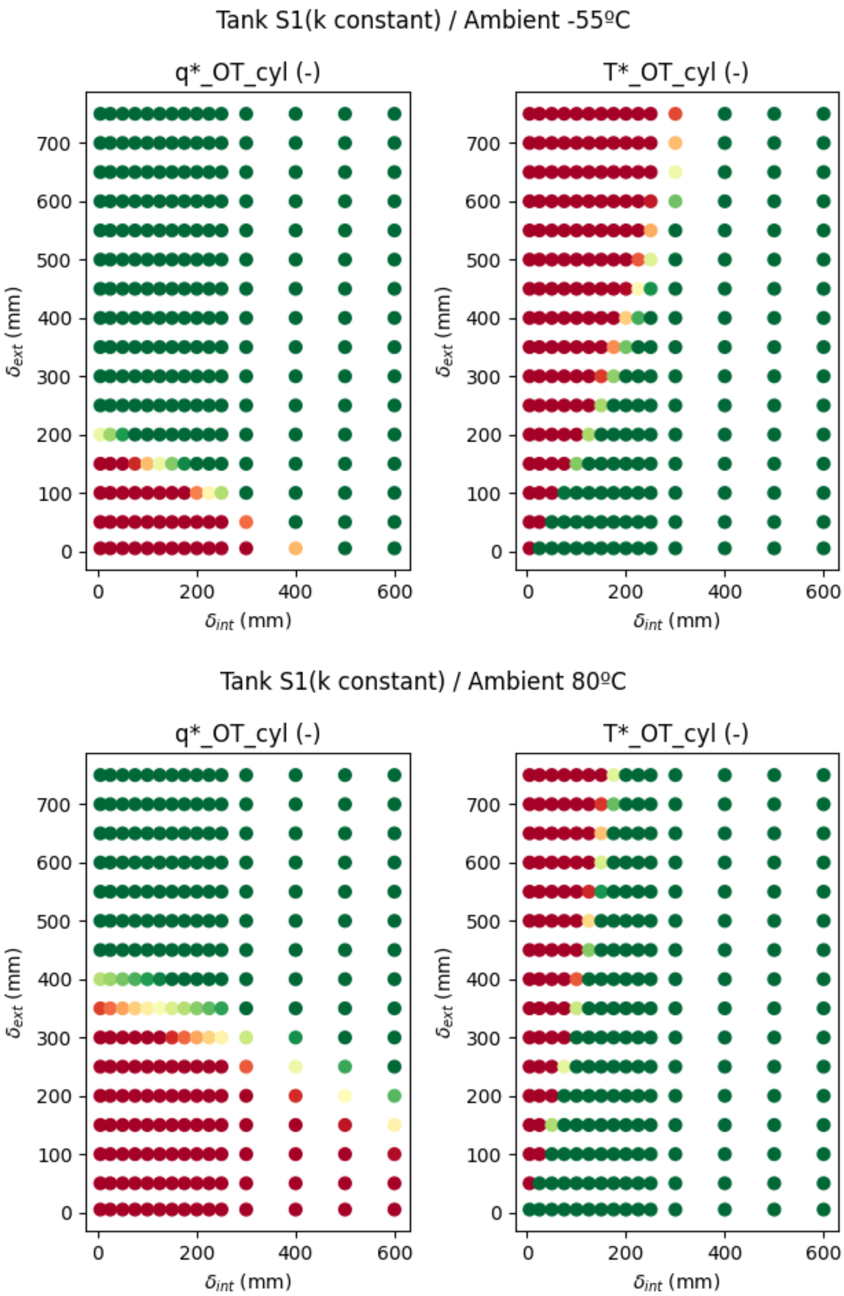

Figure 5: Areas fulfilling (green) or not (red) the limits for heat flux (left) and outer tank temperature (right). Values shown for minimum (top) and maximum (bottom) ambient temperatures.

it comes as an output of a particular illustrative case, and second, it implies the need for additional internal project design iterations before concluding about its feasibility.

3.4 Scalability insight

Taking the previous statements about the characteristics of the concept for the S1 tank, it is of even more interest to have an insight into the behaviour of the same solution for other tank sizes, assessing its scalability and technology potential. In this sense, the same procedure explained for the smallest tank (S1) has been applied for the other sizes described in Table 1. Figure 8 shows the feasible working zone for S4 and S6, adding the corresponding gravimetric parameter for each thickness combination. As observed, coming from an increased allowable heat flux ratio to keep the same dormancy times in bigger H_2 volumes, the feasible thickness combinations decrease with the tank size. Finally, the

DOI: 10.13009/EUCASS2025-170

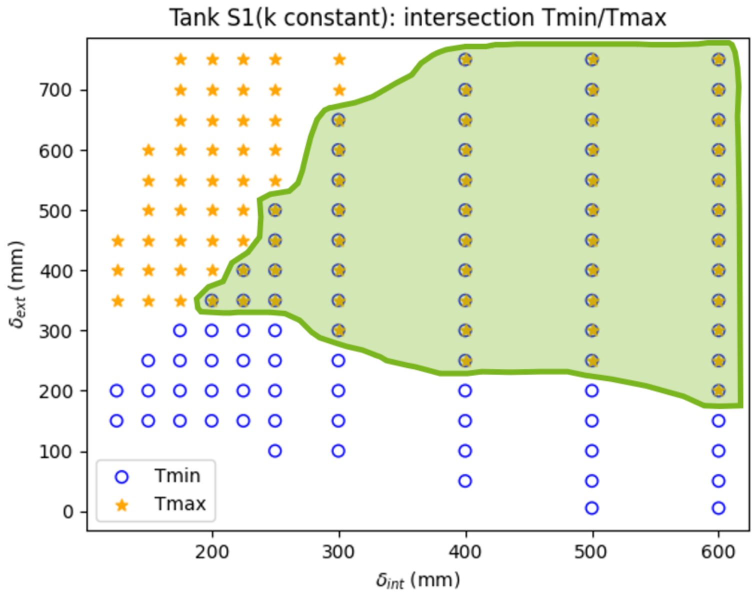

Figure 6: Composition of design zones covering simultaneously the design constraints for minimum and maximum ambient temperature conditions (green envelope).

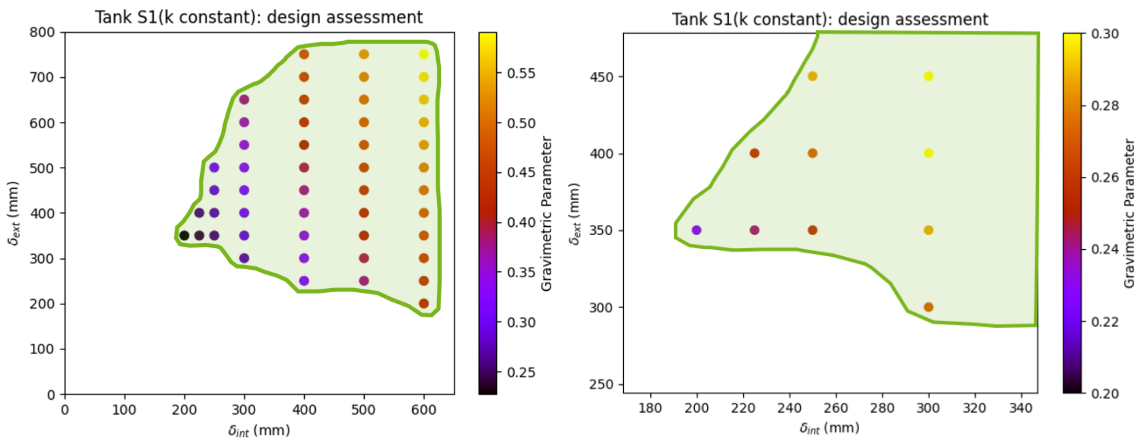

Figure 7: Design zone for S1, coloured by gravimetric parameter (left whole envelope, right zoom of the best zone).

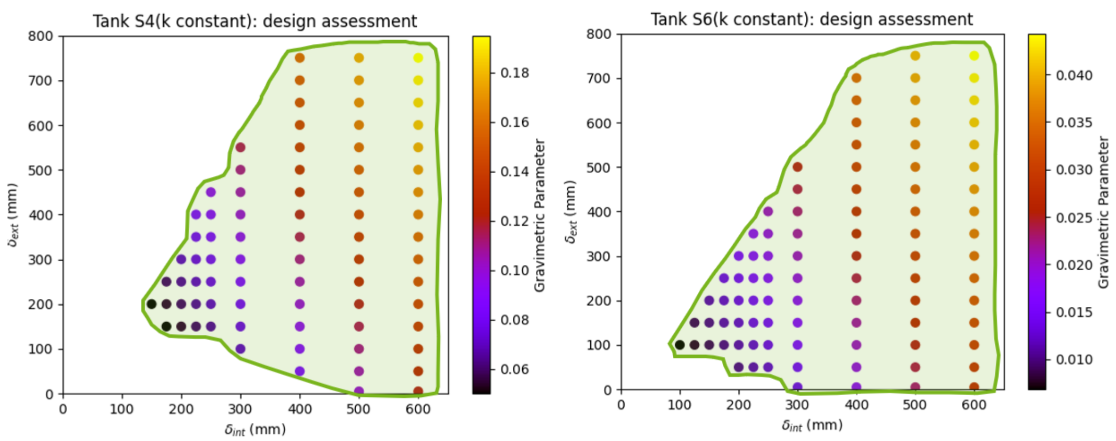

Figure 8: Design zone for S4 and S6, coloured by gravimetric parameter.

DOI: 10.13009/EUCASS2025-170

gravimetric parameter decreases substantially, widening the options to consider the dual-foam technology as a feasible alternative.

4. Conclusions

The interest towards sustainable aviation is currently driving several research activities. Hydrogen powered aircraft is one of the topics under this framework, for which lightweight and safe LH_2 storage is a key aspect. In this context, this paper focuses on reporting a methodology to assess the selection of insulation thicknesses for a dual-foam based insulation design. Dormancy target, together with safe operating temperatures at the interface between the two foams, are the baseline of the assessment. The simulations have been done for a reference tank, taking constant and illustrative properties at this stage due to confidentiality reasons. The feasible insulation thickness perimeter complying with the two mentioned restrictions has been determined. Additional KPIs for each design point can finally be added to select the best insulation (in the paper, a gravimetric parameter has been defined for this purpose). Similar results have been generated for other tank sizes to report the scalability behaviour of this dual-foam design. The methodology can therefore be applied as a pre-design tool for dual-foam LH_2 tanks, adding in the future actual material properties depending on the operating conditions and refined KPIs to assess the final design decisions.

5. Acknowledgments

Developed in the mark of the *HydrogEn Lightweight & Innovative tank for zerO-emisSion aircraft* (H2ELIOS). Clean Aviation research project Ref. 101102003 (https://h2elios.eu/home). The project H2ELIOS is supported by the Clean Aviation Joint Undertaking and its members.

Co-funded by the European Union

CLEAN AVIATION

Disclaimer: The contents presented in this article reflect only the author's point of view: the authors and Clean Sky JU are not responsible for any use that may be made of the information it contains. Funded by the European Union. Views and opinions expressed are, however, those of the author(s) only and do not necessarily reflect those of the European Union or Clean Aviation Joint Undertaking. Neither the European Union nor the granting authority can be held responsible for them.
Carles Oliet, as a Serra Húnter Associate Professor, acknowledges the Catalan Government for the support through this Program. Marcial Mosqueda-Otero is supported by the Catalan Agency for Management of University and Research Grants (2024 FI-1 00684)

References

[1] S.Z.S. Al Ghafri, A Swanger, V. Jusko, A. Siahvashi, F. Perez, M. L. Johns, and E. F. May. Modelling of liquid hydrogen boil-off. *Energies*, 15(3):1149, 2022.

[2] F. M. Anthony, J. Z. Colt, and R. G. Helenbrook. Development and Validation of Cryogenic Foam Insulation for LH_2 Subsonic Transports. Technical Report 3404, NASA, 1981.

[3] J. C. Aydellot. Normal gravity self-pressurization of 9-inch-(23 cm) diameter spherical liquid hydrogen tankage. Technical Report TN D-4171, NASA, 1960.

[4] D. Cimadevilla and J. Ortega. Cryogenic tank (European Patent EP4283182A1), May 2022.

[5] J. E. Fesmire, J B Ancipink, A. M. Swanger, S. White, and D. Yarbrough. Thermal conductivity of aerogel blanket insulation under cryogenic-vacuum conditions in different gas environments. *IOP Conf. Series: Materials Science and Engineering*, 278(012198), 2017.

[6] H. Hamori, H. Kumazawa, R. Higuchi, and T. Yokozeki. Gas permeability of CFRP cross-ply laminates with thin-ply barrier layers under cryogenic and biaxial loading conditions. *Composite Structures*, 245:112326, 2020.

[7] M. M. Hasan, C.S. Lin, and N.T. Van Dresar. Self-pressurization of a flightweight liquid hydrogen storage tank subjected to low heat flux. Technical Report Technical Memorandum 103804, NASA, 1991.

DOI: 10.13009/EUCASS2025-170

[8] L. J. Hastings, A. Hedayat, and T. M. Brown. Analytical modeling and test correlation of variable density multilayer insulation for cryogenic storage. Technical Report TM_2004_213175, NASA, 2004.

[9] E. W. Lemmon, I. H. Bell, M. L. Huber, and M. O. McLinden. NIST standard reference database 23: reference fluid thermodynamic and transport properties-REFPROP, version 10.0, national institute of standards and technology. *Standard Reference Data Program, Gaithersburg*, 2018.

[10] N. Liu, B. Ma, F. Liu, W. Huang, B. Xu, L. Qu, and Y. Yang. Progress in research on composite cryogenic propellant tank for large aerospace vehicles. *Composites Part A: Applied Science and Manufacturing*, 143:106297, 2021.

[11] S. K. Mital, J. Z. Gyekenyesi, S. M. Arnold, R. M. Sullivan, J. M. Manderscheid, and P. L. N. Murthy. Review of current state of the art and key design issues with potential solutions for liquid hydrogen cryogenic storage tank structures for aircraft applications. Technical Report ID 20060056194,, NASA, 2006.

[12] C. Oliet, M. Mosqueda-Otero, E. Schillaci, A. Amani, J. Rigola, and Jesús Castro. Thermal Digital Twin of LH2 Aircraft Storage Tank. *Engineering Proceedings*, 90(1), 2025.

[13] P. J. Sun, J. Y. Wu, P. Zhang, L. Xu, and M. L. Jiang. Experimental study of the influences of degraded vacuum on multilayer insulation blankets. *Cryogenics*, 49(12):719–726, 2009.

[14] D. Terlizzi, A. Bamoshmoosh, and G. Valenti. Review of liquid hydrogen tanks for short- and medium-haul aircraft. ECCOMAS, 2024. https://www.scipedia.com/public/Terlizzi_et_al_2024a.